Pathophysiology 26 (2019) 203–212

Contents lists available at ScienceDirect

Pathophysiology

journal homepage: www.elsevier.com/locate/pathophys

Mobile phone electromagnetic radiation affects Amyloid Precursor Protein and α-synuclein metabolism in SH-SY5Y cells

Aikaterina L. Stefi[a,b], Lukas H. Margaritis[b], Aikaterini S. Skouroliakou[c], Dido Vassilacopoulou[a,*]

[a] Department of Biochemistry and Molecular Biology, Faculty of Biology, National and Kapodistrian University of Athens, Athens, 15784, Greece
[b] Department of Cell Biology and Biophysics, Faculty of Biology, National and Kapodistrian University of Athens, Athens, 15784, Greece
[c] Department of Biomedical Engineering, University of West Attica, Athens, Greece

ARTICLE INFO

Article history:
Received 17 October 2018
Received in revised form 19 February 2019
Accepted 22 February 2019

Keywords:
GSM
Alzheimer
Parkinson
Neuroblastoma
ROS
Cell death

ABSTRACT

In this study, the effects of low-level, GSM emitted ElectroMagnetic Field (EMF) on Amyloid Precursor Protein (APP) and alpha-synuclein (α-syn) in human neuroblastoma cells was investigated. Our data indicated alterations on APP processing and cellular topology, following EMF exposure (ε = 10.51 V/m, SAR = 0.23 W/kg, exposure time: 3 times, for 10 min, for 2 days). Furthermore, changes in monomeric α-syn accumulation and multimerization, as well as induction of oxidative stress and cell death, were documented. The results presented here require further investigation to determine potential links of EMF with the molecular pathogenic mechanisms in Alzheimer's and Parkinson's Diseases.

1. Introduction

Radiation emitted from cellular phones has been suggested to potentially affect several health issues [1]. Several studies reported evidence for headaches and sleep perturbations [2], blood brain barrier's disturbances [3], and even genetic and proteomic alterations in humans [4,5]. *In vitro* studies have demonstrated that Extra Low Frequency – ElectroMagnetic Field (ELF-EMF) exposure might affect modulation of heat shock proteins, apoptosis and DNA damage [6–9]. A recent survey by IARC (International Agency for Research on Cancer, an agency within the World Health Organization) has classified radiation emitted by mobile phones and related devices, as a probable human carcinogen (2B category) [10,11]. Effects of non-ionizing radiation have also been described in other organisms. These include alterations on reproduction and development [12,13,14], cognitive and memory dysfunctions [15], oxidative stress induction [16–18] and apoptosis [19,20]. Recently, EMF exposure has been shown to cause developmental effects in plants [21–25].

Neurodegenerative disorders such as Alzheimer's Disease (AD) and Parkinson's Disease (PD), are characterized by the progressive degeneration of the Central Nervous System (CNS). AD is known to lead to progressive mental, behavioral and functional decline [26]. It is estimated that approximately 10% of the global population over the age of 60 and 50% over the age of 85 is affected by AD [27], a fact having an enormous global and social economic impact [28]. Extracellular brain depositions of Amyloid ß (Aß) peptide are considered to be the histopathological hallmark of AD. This process leads to neuritic plaque formation in the Central Nervous System (CNS). Aß peptide is generated by the proteolytic processing of Amyloid Precursor Protein (APP). APP is a type I transmembrane glycoprotein [29–32]. The APP Aß sequence includes the 28 terminal amino acids of the extracytoplasmic region of the precursor and 12–15 residues of the transmembrane sequence of APP. The generation of Aß peptide is the result of APP proteolysis by β -and γ-secretases [33].

PD is caused by the degeneration of dopaminergic neurons in the *substantia nigra* [34]. The main histopathological characteristic of PD is the formation of Lewy bodies (LB) in pigmented brainstem

Abbreviations: AD, Alzheimer's Disease; APP, Amyloid Precursor Protein; Aß, beta amyloid peptide; CNS, Central Nervous System; D, Down configuration cell culture; ELF, ExtraLow Frequency; EMF, ElectroMagnetic Field; EMR, ElectroMagnetic Radiation; GSM, Global System for Mobile communications; IARC, International Agency for Research on Cancer; ICNIRP, International Commission on Non-Ionizing Radiation Protection; LB, Lewy Body; PD, Parkinson's Disease; RF, RadioFrequency; ROS, Reactive Oxygen Species; SAR, Specific Absorbance Rate; U, Up configuration cell culture; α-syn, alpha synuclein.

* Corresponding author.
E-mail address: didovass@biol.uoa.gr (D. Vassilacopoulou).

https://doi.org/10.1016/j.pathophys.2019.02.004
0928-4680/

nuclei [35]. Alpha synuclein (α-syn) is a 140-amino acid, natively unfolded, presynaptic neuronal protein composed of three distinct domains [36]. It has been suggested that in normal brain tissue, α-syn controls dopamine levels by decreasing dopamine transporter activity [37]. Alpha synuclein aggregates are considered to represent the major component of LBs, although the precice LB biochemical composition remains unclear. Free radicals generated by dopamine metabolism are proposed to enhance α-syn neurotoxicity in dopaminergic neurons [38]. Oligomeric toxic protofibrils of α-syn have been implicated in the disruption of cellular homeostasis leading eventually to neuronal death followed by a total failure of synaptic function [39].

Studies on the effects of electromagnetic radiation (EMR) in AD pathogenesis, have produced conflicting evidence. Epidemiological studies suggested that frequent EMF exposure may lead to a significant higher risk for the development of AD [40,41]. It has been suggested that exposure to non-ionizing EMF could affect peripheral or neuronal processing of APP in humans [42]. *In vivo* studies on rats exposed to EM pulsed field (field strength 50 kV/m, repetition rate 100 Hz), demonstrated long-term impairment in cognition and memory [43].

On the contrary, it has been reported that exposure of advanced AD mouse models to EMF, for 8 months (1950 MHz, Specific Absorbance Rate – SAR- 5 W/kg, 2 h/day, 5 days/week) attenuates the development of further AD-like pathology. Jeong and his collagues [44] concluded that radio frequency - RF-EMF exposure can have a beneficial influence on pre-existing AD in mice. Arendash et al., [45] suggested that EMF could have beneficial effects on cognitive impairment in AD transgenic mice, mainly via mitochondrial function enhancement due to EMF exposure [46]. As far as the effect of non-ionizing EMF on PD pathogenesis is concerned, only a few pieces of evidence are available [47,48].

Since very little is known about the effects of the non-ionizing radiation-emitting devices on the biochemical processes leading to the pathogenesis of AD and PD, the current investigation focuses on APP and α-syn metabolism, following EMF irradiation in human cells of neuronal origin.

2. Experimental procedure

2.1. Cell culture

The SH-SY5Y human neuroblastoma cell line, obtained from ATCC®, was cultured in Dulbecco's Modified Eagle's Medium (DMEM, PAA Laboratories™ E15-009). These cells have been used as a model for the study of neurodegenerative diseases [49]. Cell medium was supplemented with 10% heat-inactivated Fetal Bovine Serum Fetal Bovine Serum (FBS Gibco™, 10500064) and 100 U/ml penicillin/streptomycin (Gibco™, 15140122). Cell cultures were maintained in a humidified atmosphere of 5% CO_2 at 37 °C (SANYO™ CO_2 Incubator, model MCO-15AC-Sanyo Electric Co Ltd) and medium was replenished three times per week.

2.2. Experimental setup

Same passage SH-SY5Y cells (P8-P15) were irradiated using a GSM (Global System for Mobile communications) 1800 MHz mobile phone (Motorola C123, Motorola, Inc. Chicago, Illinois) in talking mode. The entire experimental setup is depicted in Fig. 1a. The emitting cellular device was placed between two culture flasks (Sarstedt Inc, T75 TC FLASK, 50-809-260), which were designated as **down (D)** and **up (U)** cultures accordingly (Fig. 1). Cells were irradiated for 10 min within the laminar flow hood in the presence of a cellular phone. The experimental setup included a portable AM/FM radio apparatus (Panasonic, RF-H 830) in order to simulate talking mode.

To investigate any possible thermal effects of the emitted radiation, a two channel industrial Data Logging (Model AZ9882) printing thermometer (Probe sensitivity: approximately 43 μV/°C) was employed to measure temperature changes. Ten minutes before exposure, one sterilized Type T (copper–constantan) needle shaped, thermocouple was submerged in the culture medium of each of the two experimental cell cultures. Before, during and ten minutes after irradiation, the temperature of the culture medium was measured, for each of the experimental cultures. The two channel records were printed, every 30 s, through a built-in printer.

After the 10-minute exposure, D and U configuration cell cultures were placed in the incubator. The sham-exposed cultures were treated for 10 min in the same laminar flow hood, under identical conditions, while turning the cell phone off. The exposure procedure was repeated twice; for a total of three times within 24 h separated by 2 h intervals. The exposure procedure was performed for a total of 2 days. Twenty-four hours following the last irradiation protocol, cells were collected for cell death measurements, Reactive Oxygen Species (ROS) estimation or storage at −18 °C for further SDS-PAGE and Western blotting analyses.

The average electrical field intensity was measured for 6 min according to ICNIRP guidelines [50]. Two spectrum analyzers NARDA SRM3000 (NARDA Safety Test Solutions, Inc., Mönchengladbach, Germany) and ROHDE & SCHWARZ FSL/6 (with near field probes, by Langer, EMV-Technik GmbH, Germany) were used. Cell culture electrical field intensity, specifically measured within the culture medium, was significantly different for each of the two culture flasks; i.e. 10 V/meter for the culture medium at the upper flask, adjacent to the keyboard side of the phone (**U** orientation during exposure) and 3.5 V/meter for the culture medium of the lower flask, (**D** orientation during exposure). The SAR for DMEM, calculated according to Schuderer et al., [51] ($\sigma = 2.1$ S/m, $\rho = 1000$ kg/m^3), was equal to 0.21 W/kg for the **U** orientation and 0.026 W/kg for the **D** orientation. This difference is due to the culture flask configuration. The culture in the **U** configuration, was in contact with the flask wall adjacent to the cellular phone, while the culture of the **D** configuration sustained lower EMF radiation intensity since not only the upper flask wall but also an approximately 30 mm-thick air layer intervened, between the culture medium and the emitting cellular phone. Continuous monitoring of the E-field intensity was recorded via suitable software (Smartfield meter-EMC test design LLC, Mass., USA).

2.3. Antibodies

Anti-APP antibodies were raised in the laboratory of Dr. D. Vassilacopoulou against the Aß peptide of human APP, as well as, the C-terminal region of the protein. All reagents used were of analytical grade. The antibody against human α-syn (MFCD02095740 - S3062) and the secondary antibody (MFCD00162782) were purchased from Sigma-Aldrich™, Milan, Italy.

2.4. Temperature-induced phase separation in Triton X-114

Phase partition was performed according to the method of Bordier, [56]. The non-ionic detergent Triton X-114 (Sigma-Aldrich™, Milan, Italy, 9036-19-5) was pre-condensed in order to remove possible hydrophilic contaminants. Proteins extracted from cell cultures from both sham-exposed and exposed samples, were resuspended in ice cold TBS (10 mM Tris–HCl, 150 mM NaCl, pH 7.2). Triton X-114 was added to a final concentration of 2%. The mixture was incubated for 15 min in an ice bath with occasional mixing and then centrifuged in a microcentrifuge for 10 min at 4 °C and 13.000 x g. The pellet (Triton X-114 insoluble/phospholipid rich

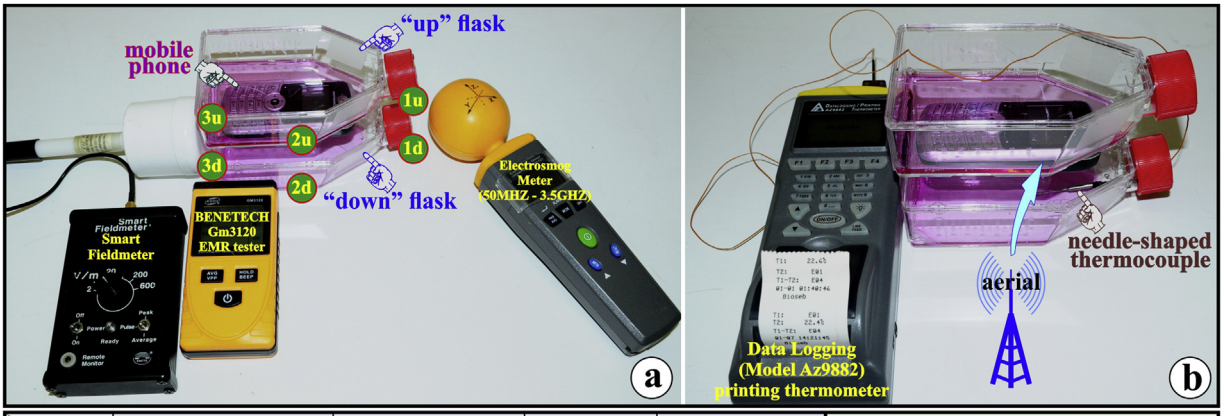

values / position	Maximum E-field intensity (V/m)	Average E-field intensity (V/m)	S A R (W/kg)	Average B-field intensity (μT)	Background values		
1u	39.64	10.51	0.23	0.99	Average E-field intensity (V/m)	0.198	laminar flow
2u	25.36	8.08	0.14	0.85	Maximum E-field intensity (V/m)	0.481	
3u	16.75	7.09	0.11	0.71	Average B-field intensity (μT)	0.41	
1d	7.82	3.50	0.026	0.62	Average E-field intensity (V/m)	0.156	culture chamber
2d	6.52	2.71	0.015	0.55	Maximum E-field intensity (V/m)	0.252	
3d	3.75	2.01	0.008	0.49	Average B-field intensity (μT)	0.21	c

Fig. 1. Experimental set-up.
a) The mobile hand set was placed between the two test cell cultures. The instrumentation used to monitor and record the emitted radiation surrounding the upper culture flask (1u, 2u, 3u test points), as well as the lower culture flask (1d, 2d, 3d test points) are depicted. **b)** The digital thermometer readings were obtained by means of the needle-shaped probe which was submerged in the culture medium of the lower culture flask. The arrow indicates the position of the handset antenna. **c)** Values of EMR intensity and SAR were recorded in different positions surrounding the upper and the lower culture flasks. Background values are given on the right side of the table.

phase), the upper phase (detergent-depleted) and the lower phase (detergent-enriched) were subjected to western blotting analyses.

2.5. Protein extraction and western blot analysis

Protein extraction was performed using RIPA lysis buffer (Thermo Fisher Scientific Inc. – NYSE: TMO, 89900). Samples were centrifuged (12.000 x g, 10 min, 4 °C, for 3 times) and the supernatants were stored at −20 °C.Total protein concentration was determined according to the method of Bradford [52], using bovine serum albumin as standard. SDS-polyacrylamide gel electrophoresis and immunoblotting SDS-PAGE was performed on a "Biorad Mini Protean" electrophoresis apparatus as described by Laemmli [53], using both 8% and 15% polyacrylamide slab gels. Electrophoresis was performed at 70 V for 5 h at room temperature. Following electrophoresis, samples were transferred onto nitrocellulose [54]. Immunological detection was performed according to the method of Batteiger [55] and subsequent immunological detection was performed using the polyclonal antibodies described above. Quantification of bands of immunodetections was performed using the software "Image Pro Plus" v.10.0 and the derived data were illustrated in bar graphs using "OriginLab Pro" v.9.0.

2.6. ROS measurements

ROS levels were measured using 10 mM of the oxidant sensitive fluorescent acetyl ester CM-H_2DCFDA (5 -(and-6)-chloromethyl-2′,7′–dichloro-dihydro-fluorescein diacetate - Thermofischer Scientific™, C6827) dissolved in DMSO (Sigma-Aldrich, Milan, Italy, 67-68-5). CM-H_2DCFDA is an oxidative stress indicator that moves through the cell membrane by passive diffusion. Inside the cell the ester's acetate groups are cleaved by intracellular esterases and oxidation by ROS leads to the formation of the fluorescent DCF product, which can be detected via fluorometry. The procedure used was as follows: Cells were collected via trypsinization and centrifugation at 1450 rpm for 5 min. Subsequently, samples were incubated continuously for 30 min in the presence of CM-H_2DCFDA diluted in serum free medium at 37 °C. The ester was subsequently removed, prior to further incubation, for 20 min in serum free medium. Cells were washed three times with PBS buffered solution and centrifuged for 5 min. The obtained supernatant was used for fluorescent measurements in a Versa Fluor Fluorometer System (Bio-Rad™, 170- 2402, Hercules, CA). The excitation filter was set at 490 nm and emission at 520 nm. Each set of experiments was performed in duplicates. Total ROS was expressed as fluorescent units/μg of protein extracts.

2.7. Cell death measurements

Trypan blue exclusion method was employed for cell death measurements following exposure sessions. Results were expressed as the mean of three independent experiments. Cytotoxicity was calculated according to the following [57].

$$\%\,Dead = \frac{Number\ of\ colorless\ cells}{Total\ number\ of\ cells} \cdot 100$$

2.8. Statistical analysis

Results were analyzed using the SPSS v.21.0 software (SPSS Inc., Chicago, IL). Differences in mean scores were analyzed using one-way analysis of variance (ANOVA). Statistical analysis was performed by employing separate t-tests comparing the sham-exposed group to each one of the exposed groups. Data were expressed as mean ± S.D. and evaluated by Student's *t*-test. The

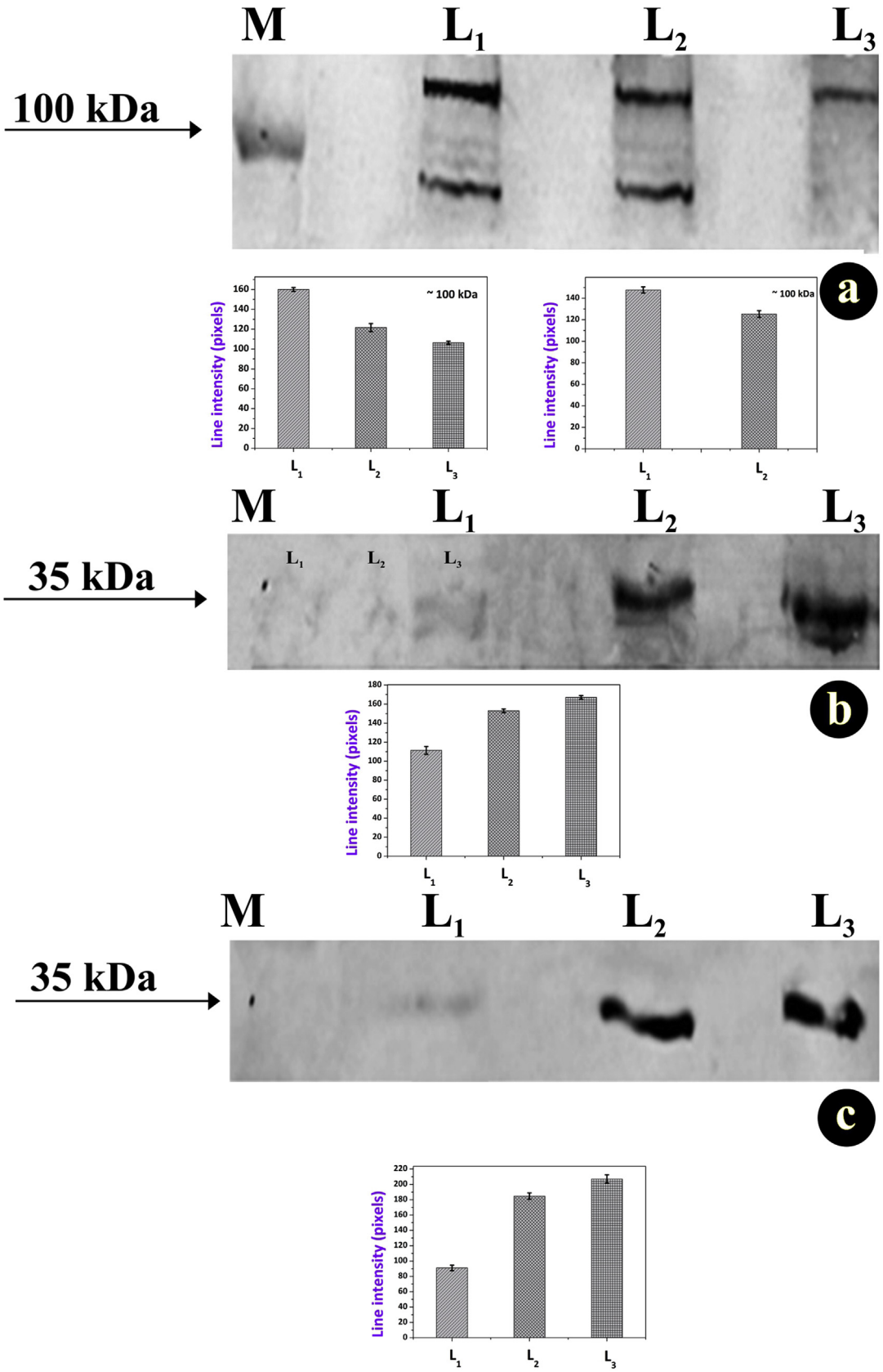

Fig. 2. Effect of non-ionizing exposure on APP metabolism.
Panel (a), **Panel (b)**: Immunodetection was carried out using the anti-Aß specific antibody. **Panel (c)**: Immunodetection using the APP anti-C-terminal specific antibody. *(M: MW marker; L_1: sham exposed cells; L_2: exposed cells in D configuration; L_3: exposed cells in U configuration).* Immunodetection quantification is illustrated in bar graphs below each panel.

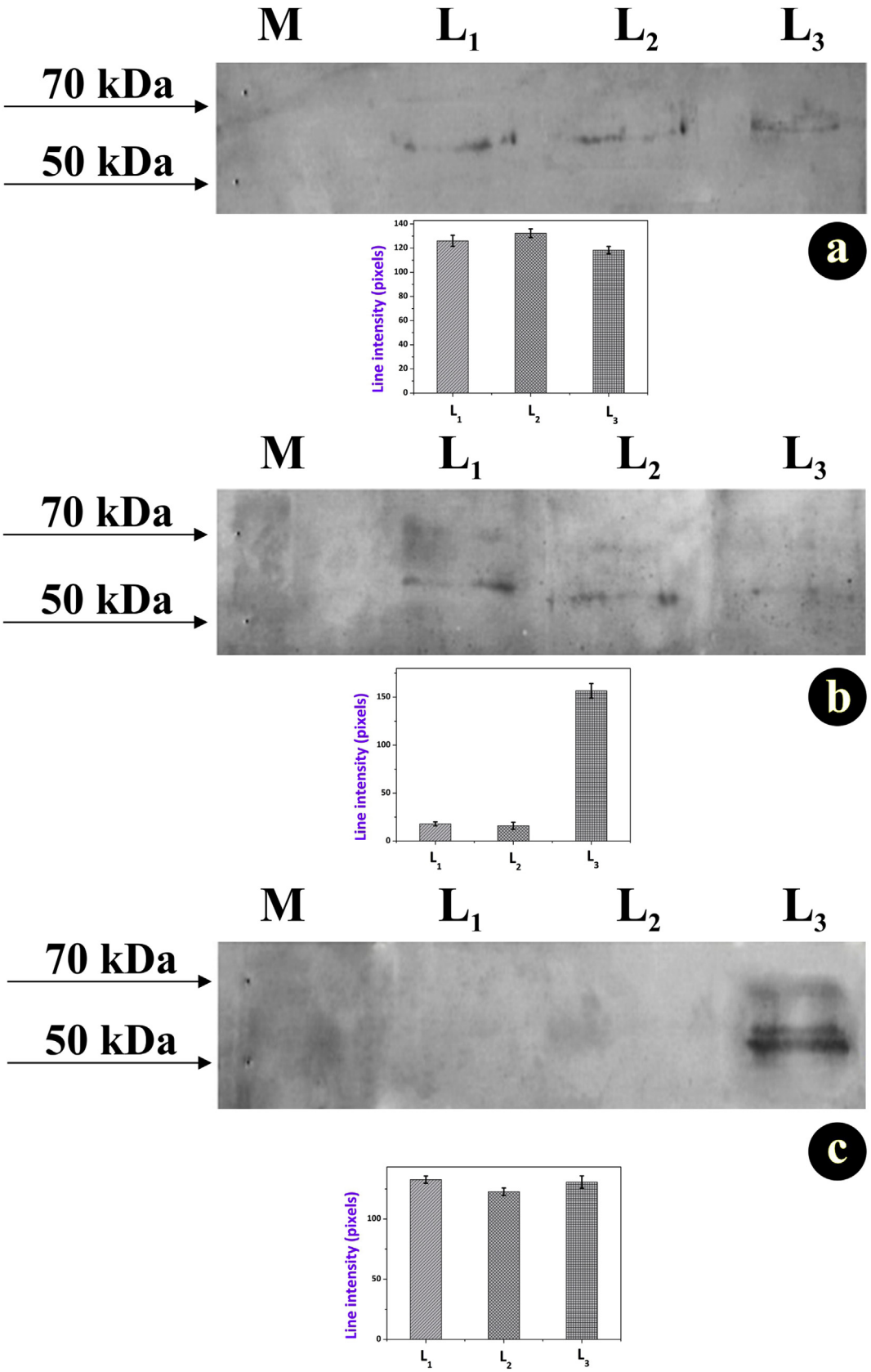

Fig. 3. Triton X-114-Temperature-induced phase separation.
Panel (a): Immunodetection of APP amyloidogenic fragments; Triton X-114 detergent-enriched phase, **Panel (b)**: Immunodetection of APP amyloidogenic fragments; Triton X-114 insoluble (phospholipid-enriched) phase, and **Panel (c)**: Immunodetection of APP amyloidogenic fragments; Triton X- 114 detergent-depleted (aqueous) phase. (*M: MW marker; L_1: sham-exposed cells; L_2: exposed cells in D configuration; L_3: exposed cells in U configuration*). Immunodetection quantification is illustrated in bar graphs below each panel.

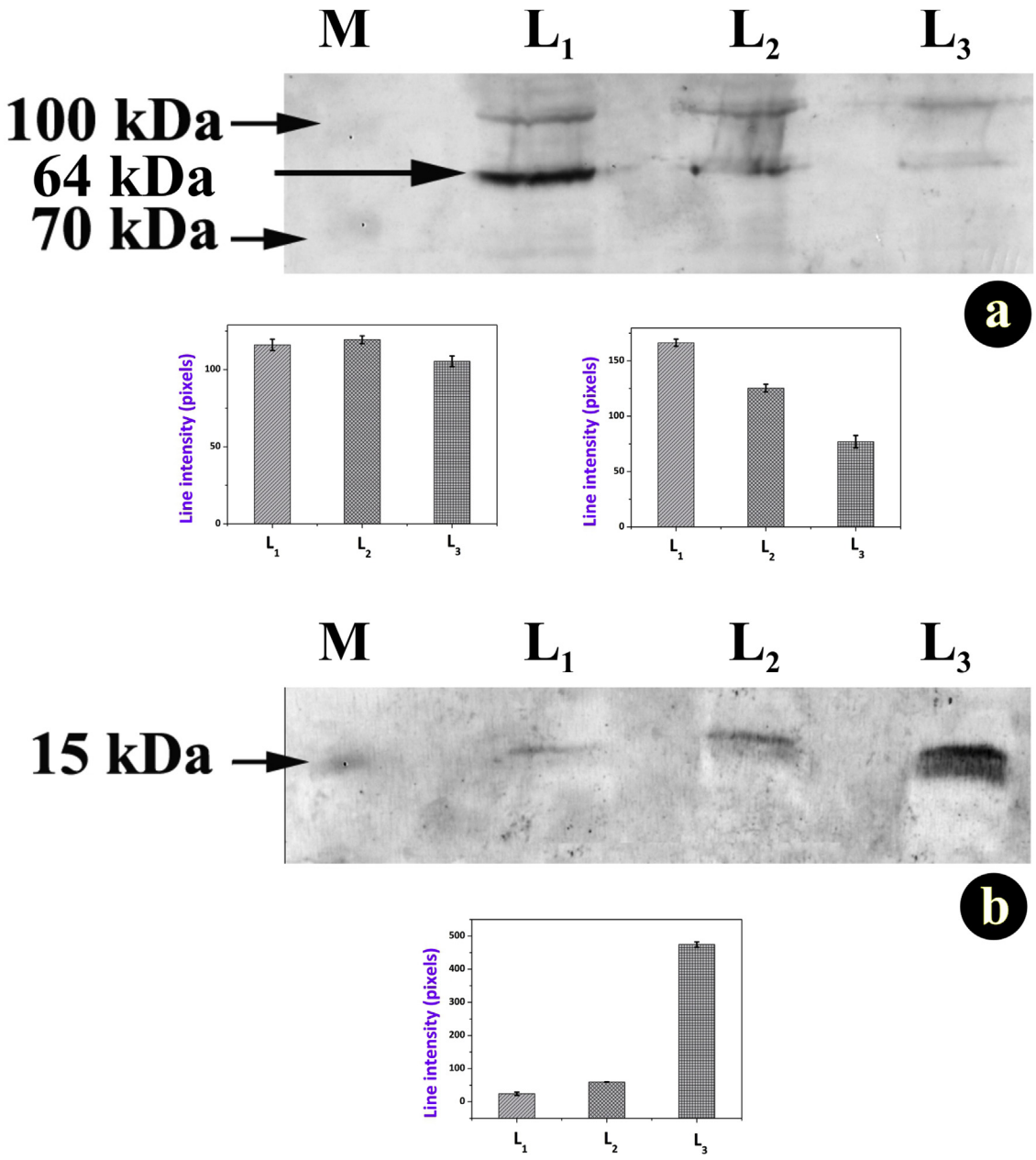

Fig. 4. Effect of non-ionizing radiation on α-synuclein metabolism.
Immunodetection was carried out using the anti-α-synuclein specific antibody. *(M: MW marker; L_1: sham-exposed cells; L_2: exposed cells in D configuration; L_3: exposed cells in U configuration).* Immunodetection quantification is illustrated in bar graphs below each panel.

differences were considered to be statistically significant when $p < 0.05$.

3. Results

3.1. Effect of non-ionizing electromagnetic radiation on APP metabolism

In an effort to study possible effect of non-ionizing electromagnetic radiation on APP metabolism, APP fragments containing the Aß and C-terminal epitopes on both sham-exposed and experimental cell cultures were detected by immunostaining using the anti-Aß and anti-C-terminal APP polyclonal antibodies (Fig. 2), as described in the Methods section. Exposure of SH-SY5Y cells to mobile phone EMF (GSM 1800 MHz), causes altered APP metabolism in Western blot analyses, as compared to the sham-exposed samples. Aß immunostaining of SH-SY5Y cell homogenates revealed that the high molecular weight Aß reactive APP species (~120 kDa), is significantly decreased in exposed samples. D configuration and sham-exposed samples demonstrated comparable levels of ~80 kDa Aβ epitope-containing APP fragments. On the other hand, in U configuration exposed samples the corresponding fragment was not detectable (Fig. 2a). In both irradiated cultures, a prominent amyloidogenic fragment of approximately 35 kDa was detected (L_2, L_3 in Fig. 2b). Our data indicated a 3-fold increase in the ~35 kDa Aβ immunoreactive fragment in the U configuration sample, as compared to the D configuration samples. It is noted that this ~35 kDa fragment, is barely detectable in sham-exposed samples (L_1 in Fig. 2b). The data support the concept that mobile phone EMF exposure alters the proteolytic processing of APP in exposed samples leading to the generation of new APP amyloidogenic fragments. Consequently, our results support

the modification of APP metabolism, following exposure to EMF. Furthermore, experimental data presented in Fig. 2c indicated a marked accumulation of ~35 kDa C-terminal reactive fragments in the irradiated samples (D and U configuration), as compared to sham-exposed samples. It is noted that the C-terminal staining fragment profile (L_1 in Fig. 2c) was similar to the one observed for Aß staining (L_1 in Fig. 2b). It is therefore possible that the new EMF-induced APP fragments, contain both the Aβ and C-terminal APP epitopes.

3.2. Effect of EMF exposure on APP cellular topology

In order to investigate possible alterations in the cellular topology of APP amyloidogenic fragments generated by EMF, the Triton X-114 phase separation protocol was employed. Samples were subjected to Western Blot analysis using the anti-Aß specific antibody (Fig. 3). Cell homogenates were treated with Triton X-114 to separate proteins according to their relative hydrophobicity [79]. Fig. 3, panel (a), depicts Aß reactive APP fragments recovered in the detergent-enriched phase. Panel (b) shows Aß reactive APP fragments recovered in the highly-hydrophobic phase, while panel (c) demonstrates the detection of Aß containing APP fragments in the hydrophilic phase. These data demonstrate the partition of the U configuration exposed samples in the highly-hydrophobic/phoshpolipid-enriched phase, indicating changes in cellular topology. APP amyloidogenic fragments generated following irradiation with mobile phone EMF, possess an alternative cellular topology as compared to D configuration and sham-exposed samples. It is noted that U-exposed samples were subjected to higher field intensity (Fig. 3c). This new alternative topology could create a new subcellular environment that possibly imposes novel molecular interactions to the generated APP amyloidogenic fragments.

3.3. Effect of EMF exposure on α-synuclein metabolism

Our investigation revealed a marked alteration on the profiles of α-syn monomers, as well as α-syn multimers (Fig. 4). Specifically, α-syn immunostaining revealed that in sham-exposed samples, α-syn is abundant in its tetrameric (~68 kDa) form (Fig. 4a). Alpha-synuclein multimeric form immunostaining decreases, following irradiation in both D and U- exposed samples with the loss of α-syn tetramer detection being more prominent in the U configuration samples. Furthermore, reduction in α-syn immunodetection was observed in the octameric form of α-syn (~100 kDa), which remains detectable in the D configuration experimental samples and sham-exposed samples (Fig. 4a). These data indicate an impressive increase of α-syn monomeric forms (~16 kDa) in the U configuration homogenates (Fig. 4b). Although monomeric α-syn is barely detectable in sham-exposed samples, there is an observed increase of the monomeric form in the D configuration cells and a further, ~20 fold increase of α-syn immunodetection in U configuration samples (Fig. 4b). This data indicate that exposure to EMF results in a transition of α-syn multimeric form into the monomeric form. These results suggest that EMF exposure can shift the equilibrium between α-syn monomers and multimers towards the monomeric form. Interestingly, the ~100 kDa α-syn multimers seem to have an equal distribution in the D configuration and sham-exposed samples, while there was an observed marked decrease in α-syn multimeric immunodetection in U configuration exposed samples.

3.4. ROS measurements and cell death

Our results revealed evidence for the induction of oxidative stress, following exposure to EMF as evaluated by ROS measurements. D configuration-exposed samples demonstrated a 1,5-fold increase (1,5x) in ROS content, while in U configuration-exposed samples the increase was estimated to about 2-fold (Fig. 5). These findings appear to confirm the positive correlation between EMF exposure and the induction of oxidative stress. Furthermore, EMF exposure seems to significantly increase cell toxicity. Our data indicated a marked increase in cell death for D configuration irradiated cells and U configuration irradiated cells, as compared to sham-exposed samples (Fig. 6).

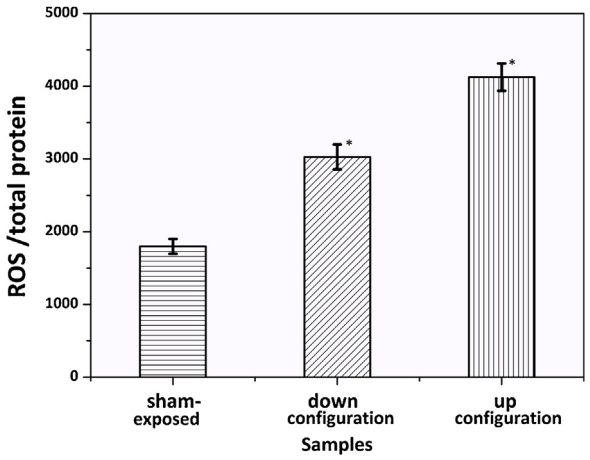

Fig. 5. The effect of mobile phone radiation on oxidative conditions.
Bar graph showing ROS levels, normalized in percentage compared to the sham-exposed values. Results were expressed as the mean ± SD from three independent experiments. Comparisons were made between sham-exposed and irradiated cultures using Student's paired *t*-test where significance was recorded as $p < 0.05$ (*).

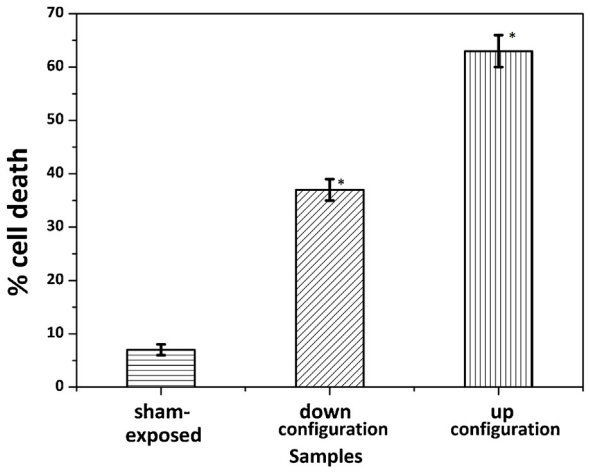

Fig. 6. Effects of mobile phone radiation on cell death.
Bar graph showing the % cell death of exposed samples compared to the sham-exposed values. Results expressed as the mean ± SD from three independent experiments. Comparisons were made between sham-exposed and irradiated cultures using Student's paired *t*-test where significance was recorded as $p < 0.05$ (*).

4. Discussion

4.1. Effect of EMF exposure on APP proteolytic processing and α-synuclein metabolism in SH-SY5Y cells

The data presented here suggest that non-ionizing electromagnetic radiation generated by a mobile phone, alters APP processing. Moreover, SH-SY5Y cells demonstrated differentiated human α-syn metabolism pattern following exposure. SDS – PAGE and western blot analyses revealed both the generation of new amy-

loidogenic APP fragments (Fig. 2b) and the corresponding reduction in full length APP immunostaining in the exposed samples from the U irradiated cultures (Fig. 2a). In the implemented experimental set-up, the thermal effects were directly and absolutely excluded since temperature was recorded to range between 22,2 °C and 22,3 °C, ten minutes before, during exposure and ten minutes following exposure (Temperature of the mobile phone was also measured during irradiation and was found to range to range between 22,5 °C and 22,6 °C.) [58,59]. The amount of energy received by the two cultures types (U and D configuration) was not identical. Exposed cells, in the U configuration, received increased electric field intensity as compared to the D configuration culture (see Table in Fig. 1c). This difference was attributed to the experimental set-up. The cell culture in the U flask was in contact to the flask wall adjacent to cellular phone. The culture of the D configuration flask sustained lower EMF radiation intensity due to the following layer interventions: 1) the flask's upper wall; 2) the $\tilde{3}$0 mm thick air layer and 3) the approximately 6 mm layer of the culture medium thickness. These layers intervened between the cells under exposure and the emitting cellular phone.

The difference in the amount of EMF energy received by the two types of cultures, might explain the observed differences in APP immunostaining pattern and proteolytic processing between the U and D irradiated cultures. Furthermore, this observation could imply a correlation between the intensity of the field and the alterations in amyloidogenic APP processing. Immunodetection of proteolytic fragments, using the specific antibody raised against the C-terminal APP region (Fig. 2c), revealed similar results. Our findings indicated that the profile of C-terminal immunoreactive APP proteolytic processing in irradiated samples (U and D cultures) was modified, demonstrating an apparent accumulation of APP C-terminal fragments. It is possible that among the accumulated Aβ immunoreactive fragments the APP C-terminal domain is included (Fig. 2b; c). Carboxy-terminal APP fragments have been shown to have a possible role in AD neuropathology due to their toxicity to neurons [60,61]. In addition, it has been reported that the APP C-terminal domain has a catalytic role in cell cycle regulation and cell differentiation processes [62]. Fragments generated by APP physiological proteolytic processing have been implicated in several different cellular functions. For example, sAPPα stimulates neuronal proliferation and protects neurons against excitotoxicity. sAPPβ has been found to be neurotrophic stimulating axonal outgrowth [62]. The C-terminal APP C99 fragment, interacts with signaling molecules that are involved in cellular differentiation pathways, such as Shca and Dab-1 [63,64]. The soluble intracellular domain of APP (AICD) has been shown to affect transcription regulation [62,65]. Our results showed that $\tilde{3}$5 kDa amyloidogenic fragments are generated following irradiation. These fragments, according to above data, could represent APP proteolytic products which are generated in response to EMF irradiation. This may represent one of the cellular responses that can be induced by EMF exposure, and include ROS formation and cell stress/death.

The results from the phase separation experiments using the Triton –X 114 method, indicated the recovery of APP amyloidogenic proteolytic products in the phospholipid-enriched separation phase (Fig. 3, panel b; L_3). This observation implies an alteration of APP amyloidogenic fragment cellular topology following irradiation. Subcellular localization is critical for the development of the APP interaction network [66–69]. Therefore, it is possible that EMF exposure might alter APP functions associated with cellular topology.

The hallmark of PD is the accumulation of α-syn insoluble aggregates within Lewy bodies [35]. Our results indicated that, in sham-exposed samples α-syn was detected mainly in its multimeric form (Fig. 4a). This observation is in agreement with recent reports suggesting that α-syn is physiologically detected mainly as a multimer. [70–73]. Bartels et al., in 2011 [70] as well as Dettmer et al., 2013 [73], proposed that multimers and monomers of α-syn co-exist in a dynamic equilibrium in healthy cellular populations. The obtained results of the current investigation agree to the findings indicating that exposure to non-ionizing EMF and the subsequent induction of oxidative stress can shift the equilibrium from multimers to the impressively increased monomers of α-syn. The observed increase of monomeric α-syn in addition to the simultaneous decrease of the 64 kDa multimer also agrees to recent reports [70,72,73]. The current results indicate that the appearance of monomers of α-syn co-exist with increased ROS levels and cellular death. It has been reported that multimeric destabilization could be triggering mechanism leading to PD [74]. A disturbance in the tetramer to monomer α-syn ratio has also been reported in familial PD cases [72]. Our data provide evidence that exposure of SH-SY5Y cells to EMF, shifts the balance towards the monomeric α-syn form. This α-syn configuration has been related to the neurotoxic events connected with PD pathogenetic mechanisms [75,76].

4.2. Effect of EMF on ROS and cell death

EMF exposure resulted in increased ROS levels (Fig. 5). ROS are normally produced throughout cell, via normal physiological metabolic processes. Yet, various environmental or chemical stressing conditions may lead to increased production of ROS [17,25]. Many studies have demonstrated that oxidative stress, is mainly caused by mitochondrial dysfunction [75–77], and has a crucial role in the pathophysiology of neurodegeneration [78–82]. Increased ROS production results in oxidative damage which causes a wide range of cellular responses ranging from proliferation induction to cell death. Experimental data from different biological systems, such as human spermatozoa [83], earthworms [84], rats [16] even in plant systems and young pines [24] have shown that exposure to EMF resulted in increased ROS levels. Human astrocytes have been demonstrated to exhibit increased ROS levels and DNA fragmentation following exposure to pulsed 900 MHz EMF [85], while exposure of SH-SY5Y cells to EMF 1800 MHz also resulted in increased ROS levels and mitochondrial DNA damage to [86]. SH-SY5Y cells present high metabolic rate and lack efficient defense mechanisms and are, therefore, considered to be vulnerable to oxidative damages [87].

Our investigation indicates that non-ionizing electromagnetic radiation may function as a stress factor leading to altered APP and α-syn metabolism. We provide new evidence supporting the concept that, EMF exposure may trigger the generation of novel APP amyloidogenic fragments, as well as, an increase of toxic α-syn monomers [70,73], and therefore argue that EMFs could be implicated in the underlying biochemical events leading to neurodegeneration.

5. Conclusions

To the best of our knowledge, the work presented here, seems to be the first report linking exposure to EMF emitted by a transmitting mobile phone, to altered metabolism of APP and α-syn in SH-SY5Y cells. The observed increase in monomeric α-syn along with the generation of novel amyloidogenic fragments possessing alternative cellular topology, in addition to the induction of cellular toxicity and oxidative stress, should be taken into consideration in future research aiming towards the understanding of the molecular mechanisms linking EMR to human health. It is possible that wireless communications, may represent a new factor affecting human health while exposure to these devices could be involved in pathogenic mechanisms leading to neurodegeneration.

Conflict of interest

The authors declare no conflict of interests.

Acknowledgments

This study represents part of Doctoral dissertation of Dr A. L. Stefi. A part of this research has been co-financed by the European Union (European Social Fund—ESF) and Greek National funds through the Operational Program "Education and Life-long Learning" of the National Strategic Reference Framework (NSRF)—Research Funding Program: THALES. Investing in knowledge society through the European Social Fund. UoA—MIS 375784: "Biological effects of nonionizing electromagnetic fields: a multidisciplinary approach" grant coordinated by Prof. L.H. Margaritis. We thank Mr Emmanouil Vourakis for his technical assistance.

References

[1] L. Hardell, C. Sage, Biological effects from electromagnetic field exposure and public exposure standards, Biomed. Pharmacother. 62 (2) (2008) 104–109.
[2] L. Hillert, T. Åkersted, A. Lowden, C. Wiholm, N. Kuster, S. Ebert, C. Boutry, S.D. Moffat, M. Berg, B.B. Arnetz, The effects of 884 MHz GSM wireless communication signals on headache and other symptoms: an experimental provocation study, Bioelectromagnetics 29 (3) (2008) 185–196.
[3] A. Schirmacher, S. Winters, S. Fischer, J. Goeke, H.J. Galla, U. Kullnick, E.B. Ringelstein, F. Stögbauer, Electromagnetic fields (1.8 GHz) increase the permeability to sucrose of the blood– brain barrier *in vitro*, Bioelectromagnetics 21 (2000) 338–345.
[4] J.G. Yan, M. Agresti, L.L. Zhang, Y. Yan, H.S. Matloub, Qualitative effect on mRNAs of injury-associated proteins by cell phone like radiation in rat facial nerves, Electromagn. Biol. Med. 28 (4) (2009) 383–390.
[5] M.J. Misa-Agustiño, J.M. Leiro-Vidal, J.L. Gomez-Amoza, M.T. Jorge-Mora, F.J. Jorge-Barreiro, A.A. Salas-Sánchez, F.J. Ares-Pena, E. López-Martín, EMF radiation at 2450 MHz triggers changes in the morphology and expression of heat shock proteins and glucocorticoid receptors in rat thymus, Life Sci. 127 (2015) 1–11, http://dx.doi.org/10.1016/j.lfs.2015.01.027.
[6] H. Kayhan, M.A. Esmekaya, A.S.Y. Saglam, M.Z. Tuysuz, A.G. Canseven, A.M. Yagci, N. Seyhan, Does MW radiation affect gene expression, apoptotic level, and cell cycle progression of human SH-SY5Y neuroblastoma cells? Cell Biochem. Biophys. 74 (2016) 99, http://dx.doi.org/10.1007/s12013-016-0734-9.
[7] E. Calabrò, S. Condello, M. Currò, N. Ferlazzo, D. Caccamo, S. Magazù, R. Ientile, Modulation of heat shock protein response in SH-SY5Y by mobile phone microwaves, World J. Biol. Chem. 3 (2) (2012) 34–40, http://dx.doi.org/10.4331/wjbc.v3.i2.34.
[8] S. Falone, M.R. Grossi, B. Cinque, B. D'Angelo, E. Tettamanti, A. Cimini, C.D. Ilio, F. Amicarelli, Fifty hertz extremely low-frequency electromagnetic field causes changes in redox and differentiative status in neuroblastoma cells, Int. J. Biochem. Cell Biol. 39 (11) (2007) 2093–2106.
[9] S.S. Seyyedi, H. Mozdarani, M. Rezaei Tavirani, S. Heydari, Induction of chromosomal aberrations in human primary fibroblasts and immortalized cancer cells exposed to extremely-low-frequency electromagnetic fields, Int. J. Radiat. Res. 8 (1) (2010) 25–29.
[10] L.L. Morgan, A.B. Miller, A. Sasco, D.L. Davis, Mobile phone radiation causes brain tumors and should be classified as a probable human carcinogen (2A) (review), Int. J. Oncol. 46 (5) (2015) 1865–1871.
[11] IARC monographs, IARC Classifies Radiofrequency Electromagnetic Fields As Possibly Carcinogenic to Humans, 2011, Press Release number 208.
[12] H. Nakamura, I. Matsuzaki, K. Hatta, Nonthermal effects of mobile-phone frequency microwaves on uteroplacental functions in pregnant rats, Reprod. Toxicol. 17 (2003) 321–326.
[13] Z.O. Merhi, Challenging cell phone impact on reproduction: a review, J. Assist. Reprod. Genet. 29 (2012) 293–297.
[14] L.H. Margaritis, A.K. Manta, C.D. Kokkaliaris, D. Schiza, K. Alimisis, G. Barkas, E. Georgiou, O. Giannakopoulou, I. Kollia, G. Kontogianni, A. Kourouzidou, A. Myari, F. Roumelioti, A. Skouroliakou, V. Sykioti, G. Varda, K. Xenos, K. Ziomas, Drosophila as a bio-marker responding to EMF sources, Electromagn. Biol. Med. 33 (3) (2014) 165–189.
[15] M.P. Ntzouni, A. Skouroliakou, N. Kostomitsopoulos, L.H. Margaritis, Transient and cumulative memory impairments induced by GSM 1.8 GHz cell phone signal in a mouse model, Electromagn. Biol. Med. 32 (1) (2013) 95–120.
[16] M.A. Esmekaya, C. Ozer, N. Seyhan, 900 MHz pulse-modulated radiofrequency radiation induces oxidative stress on heart, lung, testis and liver tissues, Gen. Physiol. Biophys. 30 (2011) 84–89.
[17] A.K. Manta, D.J. Stravopodis, I.S. Papassideri, L.H. Margaritis, Reactive oxygen species elevation and recovery in Drosophila bodies and ovaries following short-term and long-term exposure to DECT base EMF, Electromagn. Biol. Med. 33 (2) (2014) 118–131.
[18] B. Çiğ, M. Nazıroğlu, Investigation of the effects of distance from sources on apoptosis, oxidative stress and cytosolic calcium accumulation via TRPV1 channels induced by mobile phones and Wi-Fi in breast cancer cells, Biochim. Biophys. Acta 1848 (10) (2015) 2756–2765.
[19] G.J. Hook, P. Zhang, I. Lagroye, L. Li, R. Higashikubo, E.G. Moros, W.L. Straube, W.F. Pickard, J.D. Baty, J.L. Roti, Measurement of DNA damage and apoptosis in Molt-4 cells after *in vitro* exposure to radio frequency radiation, Radiat. Res. 161 (2004) 193–200.
[20] K. Maeda, T. Maeda, Y. Qi, *In vitro* and *in vivo* induction of human LoVo cells into apoptotic process by non-invasive microwave treatment: a potentially novel approach for physical therapy of human colorectal cancer, Oncol. Rep. 11 (2004) 771–775.
[21] A.L. Stefi, L.H. Margaritis, N.S. Christodoulakis, The effect of the non-ionizing radiation on cultivated plants of *Arabidopsis thaliana* (Col.), Flora 223 (2016) 114–120.
[22] A.L. Stefi, L.H. Margaritis, N.S. Christodoulakis, The effect of the non-ionizing radiation on exposed, laboratory cultivated upland cotton (*Gossypium hirsutum* L.) plants, Flora 226 (2017) 55–64.
[23] A.L. Stefi, L.H. Margaritis, N.S. Christodoulakis, The effect of the non-ionizing radiation on exposed, laboratory cultivated maize (*Zea mays* L.) plants, Flora 233 (2017) 22–30.
[24] A.L. Stefi, L.H. Margaritis, N.S. Christodoulakis, The aftermath of long-term exposure to non-ionizing radiation on laboratory cultivated pine plants (*Pinus halepensis* M.), Flora 234 (2017) 173–186.
[25] A.L. Stefi, D. Vassilacopoulou, L.H. Margaritis, N.S. Christodoulakis, Oxidative stress and an animal neurotransmitter synthesizing enzyme in the leaves of wild growing myrtle after exposure to GSM radiation, Flora 243 (2018) 67–76.
[26] R. Anand, K.D. Gill, A.A. Mahdi, Therapeutics of Alzheimer's disease: past, present and future, Neuropharmacology 76 (2014) 27–50.
[27] Y.W. Zhang, R. Thomson, H. Zhang, H. Xu, APP processing in Alzheimer's disease, Mol. Brain 4 (2011) 3.
[28] A. Wimo, L. Jönsson, J. Bond, M. Prince, B. Winblad, The worldwide economic impact of dementia 2010, Alzheimers Dement. 9 (1) (2013) 1–11.
[29] J. Kang, H.G. Lemaire, A. Unterbeck, J.M. Salbaum, C.L. Masters, K.H. Grzeschik, G. Multhaup, K. Beyreuther, B. Müller-Hill, The precursor of Alzheimer's disease amyloid A4 protein resembles a cell-surface receptor, Nature 325 (1987) 733–736.
[30] D. Goldgaber, M.L. Lerman, W.O. McBride, U. Saffiotti, D.C. Gajdusek, Characterization and chromosomal localization of a cDNA encoding brain amyloid of Alzheimer's disease, Science 235 (1987) 877–880.
[31] N.K. Robakis, N. Ramakrishna, G. Wolfe, H.M. Wisniewski, Molecular cloning and characterization of a cDNA encoding the cerebrovascular and the neuritic plaque amyloid peptides, Proc. Natl. Acad. Sci. U. S. A. 84 (1987) 4190–4194.
[32] R.E. Tanzi, J.F. Gusella, P.C. Watkins, G.A. Bruns, P. St George-Hyslop, M.L. Van Keuren, D. Patterson, S. Pagan, D.M. Kurnit, R.L. Neve, Amyloid beta protein gene: cDNA, mRNA distribution, and genetic linkage near the Alzheimer locus, Science 235 (1987) 880–884.
[33] P. Seubert, T. Oltersdorf, M.G. Lee, R. Barbour, C. Blomquist, D.L. Davis, K. Bryant, L.C. Fritz, D. Galasko, L.J. Thal, I. Lieberburg, D.B. Schenk, Secretion of beta-amyloid precursor protein cleaved at the amino terminus of the beta-amyloid peptide, Nature 361 (1993) 260–263.
[34] M. Spatola, C. Wider, Genetics of Parkinson's disease: the yield, Parkinsonism Relat. Disord. 20 (Suppl. 1) (2014) S35–8, http://dx.doi.org/10.1016/S1353-8020(13)70011-7.
[35] M.G. Spillantini, M.L. Schmidt, V.M. Lee, J.Q. Trojanowski, R. Jakes, M. Goedert, Alpha-synuclein in Lewy bodies, Nature 388 (1997) 839–840.
[36] L. Maroteaux, J.T. Campanelli, R.H. Scheller, Synuclein: A neuron-specific protein localized to the nucleus and presynaptic nerve terminal, J. Neurosci. 8 (1988) 2804–2815.
[37] K.Y. Little, D.P. McLaughlin, L. Zhang, P.R. McFinton, G.W. Dalack, E.H. Cook Jr, B.J. Cassin, S.J. Watson, Brain dopamine transporter messenger RNA and binding sites in cocaine users. A postmortem study, Arch. Gen. Psychiatry 55 (9) (1998) 793–799.
[38] C. Wersinger, A. Sidhu, Attenuation of dopamine transporter activity by alpha-synuclein, Neurosci. Lett. 340 (2003) 189–192.
[39] K.A. Conway, J.D. Harper, P.T. Lansbury, Accelerated in vitro fibril formation by a mutant alpha-synuclein linked to early-onset Parkinson disease, Nat. Med. 4 (11) (1998) 1318–1320.
[40] E. Sobel, Z. Davanipour, R. Sulkava, T. Erkinjuntti, J. Wikstrom, V.W. Henderson, G. Buckwalter, J.D. Bowman, P.J. Lee, Occupations with exposure to electromagnetic fields: a possible risk factor for Alzheimer's disease, Am. J. Epidemiol. 142 (1995) 515–524.
[41] E. Sobel, M. Dunn, Z. Davanipour, Z. Qian, H.C. Chui, Elevated risk of Alzheimer's disease among workers with likely electromagnetic field exposure, Neurology 47 (1996) 1477–1481.
[42] E. Sobel, Z. Davanipour, Electromagnetic field exposure may cause increased production of amyloid beta and eventually lead to Alzheimer's disease, Neurology 47 (6) (1996) 1594–1600.
[43] D.-P. Jiang, J. Li, J. Zhang, F. Kuang, H.Y. Lang, Y.F. Wang, G.Z. An, J.H. Li, G.Z. Guo, Electromagnetic pulse exposure induces overexpression of beta amyloid protein in rats, Arch. Med. Res. 44 (3) (2013) 178–184.
[44] Y.J. Jeong, G.-Y. Kang, J.H. Kwon, H.D. Choi, J.K. Pack, N. Kim, Y.S. Lee, H.J. Lee, 1950 MHz electromagnetic fields ameliorate Aβ pathology in Alzheimer's disease mice, Curr. Alzheimer Res. 12 (5) (2015) 481–492.
[45] G.W. Arendash, J. Sanchez-Ramos, T. Mori, M. Mamcarz, X. Lin, M. Runfeldt, L. Wang, G. Zhang, V. Sava, J. Tan, C. Cao, Electromagnetic field treatment

protects against and reverses cognitive impairment in Alzheimer's disease mice, J. Alzheimers Dis. 19 (2010) 191–210.
[46] N. Dragicevic, P.C. Bradshaw, M. Mamcarz, X. Lin, L. Wang, C. Cao, G.W. Arendash, Long-term electromagnetic field treatment enhances brain mitochondrial function of both Alzheimer's transgenic mice and normal mice: a mechanism for electromagnetic field-induced cognitive benefit? Neuroscience 185 (2011) 135–149.
[47] D.I. de Pomerai, N. Iqbal, I. Lafayette, A. Nagarajan, M. Kaviani Moghadam, A. Fineberg, T. Reader, S. Greedy, C. Smartt, D.W. Thomas, Microwave fields have little effect on alpha-synuclein aggregation in a *Caenorhabditis elegans* model of Parkinson's disease, Bioelectromagnetics 37 (2) (2016) 116–129.
[48] B. Benassi, G. Filomeni, C. Montagna, C. Merla, V. Lopresto, R. Pinto, C. Carmela Marino, C. Consales, Extremely low frequency magnetic field (ELF-MF) exposure sensitizes SH-SY5Y cells to the pro-parkinson's disease toxin MPP+, Mol. Neurobiol. 53 (2016) 4247, http://dx.doi.org/10.1007/s12035-015-9354-4.
[49] J. Kovalevich, D. Langford, Considerations for the use of SH-SY5Y neuroblastoma cells in neurobiology, Methods Mol. Biol. (Clifton, N.J.) 1078 (2013) 9–21.
[50] ICNIRP, Guidelines for limiting exposure to time-varying electric, magnetic and electromagnetic fields (up to 300 GHz), Health Phys. 74 (1998) 494–522.
[51] J. Schuderer, D. Spat, T. Samaras, W. Oesch, N. Kuster, *In Vitro*Exposure Systems for RF Exposures at 900 MHz, IEEE Trans. Microw. Theory Tech. 52 (8) (2012) 2067–2075.
[52] M.M. Bradford, A rapid and sensitive method for the quantitation of microgram quantities of protein utilizing the principle of protein-dye binding, Anal. Biochem. 72 (1976) 248–254.
[53] U.K. Laemmli, Cleavage of structural proteins during the assembly of the head of bacteriophage T4, Nature 227 (1970) 680–685.
[54] H. Towbin, T. Staehelin, J. Gordon, Electrophoretic transfer of proteins from polyacrylamide gels to nitrocellulose sheets: procedure and some applications, Proc. Natl. Acad. Sci. U. S. A. 76 (1979) 4350–4354.
[55] B. Batteiger, W.J. Newhall, R.B. Jones, The use of Tween 20 as a blocking agent in the immunological detection of proteins transferred to nitrocellulose membranes, J. Immunol. Methods 55 (1982) 297–307.
[56] C. Bordier, Phase separation of integral membrane proteins in Triton X-114 solution, J. Biol. Chem. 256 (1981) 1604–1607.
[57] L.C. Crowley, B.J. Marfell, M.E. Christensen, N.J. Waterhouse, Measuring cell death by trypan blue uptake and light microscopy, Cold Spring Harb. Protoc. (2016), http://dx.doi.org/10.1101/pdb.prot087155.
[58] I. Belyaev, A. Dean, H. Eger, G. Hubmann, R. Jandrisovits, M. Kern, M. Kundi, H. Moshammer, P. Lercher, K. Müller, G. Oberfeld, P. Ohnsorge, P. Pelzmann, C. Scheingraber, R. Thill, EUROPAEM EMF Guideline 2016 for the prevention, diagnosis and treatment of EMF-related health problems and illnesses, Rev. Environ. Health 31 (3) (2016) 363–397, http://dx.doi.org/10.1515/reveh-2016-0011.
[59] D. Belpomme, L. Hardell, I. Belyaev, E. Burgio, D.O. Carpenter, Thermal and non-thermal health effects of low intensity non-ionizing radiation: an international perspective, Environ. Pollut. 242 (Pt A) (2018) 643–658.
[60] K. Fukuchi, D.D. Kunkel, P.A. Schwartzkroin, K. Kamino, C.E. Ogburn, C.E. Furlong, G.M. Martin, Overexpression of a C-terminal portion of the b-amyloid precursor protein in mouse brains by transplantation of transformed neuronal cells, Exp. Neurol. 127 (1994) 253–264.
[61] B.L. Sopher, K. Fukuchi, A.C. Smith, K.A. Leppig, C.E. Furlong, G.M. Martin, Cytotoxicity mediated by conditional expression of a carboxyl terminal derivative of the b-amyloid precursor protein, Mol. Brain Res. 26 (1994) 207–217.
[62] T.E. Willnow, C.M. Petersen, A. Nykjaer, VPS10P-domain receptors - regulators of neuronal viability and function, Nat. Rev. Neurosci. 9 (12) (2008) 899–909.
[63] J. Herz, Y. Chen, Reelin, lipoprotein receptors and synaptic plasticity, Nat. Rev. Neurosci. 7 (11) (2006) 850–859.
[64] R. van der Kant, L.S. Goldstein, Cellular functions of the amyloid precursor protein from development to dementia, Dev. Cell 32 (4) (2015) 502–515.
[65] A. Nikolaev, T. McLaughlin, D.D. O'Leary, M. Tessier-Lavigne, APP binds DR6 to trigger axon pruning and neuron death via distinct caspases, Nature 457 (7232) (2009) 981–989.
[66] A.L. Barabási, Z.N. Oltvai, Network biology: understanding the cell's functional organization, Nat. Rev. Genet. 5 (2) (2004) 101–113.
[67] A. Ho, T.C. Südhof, Binding of F-spondin to amyloid-beta precursor protein: a candidate amyloid-beta precursor protein ligand that modulates amyloid-beta precursor protein cleavage, Proc. Natl. Acad. Sci. U.S.A. 101 (2004) 2548–2553.
[68] F.C. Lourenco, V. Galvan, J. Fombonne, V. Corset, F. Llambi, U. Muller, D.E. Bredesen, P. Mehlen, Netrin-1 interacts with amyloid precursor protein and regulates amyloid-beta production, Cell Death Differ. 16 (2009) 655–663.
[69] T. Serafini, S.A. Colamarino, E.D. Leonardo, H. Wang, R. Beddington, W.C. Skarnes, M. Tessier-Lavigne, Netrin-1 is required for commissural axon guidance in the developing vertebrate nervous system, Cell 87 (1996) 1001–1014.
[70] T. Bartels, J.G. Choi, D.J. Selkoe, α-Synuclein occurs physiologically as a helically folded tetramer that resists aggregation, Nature 477 (2011) 107–110.
[71] X. Wang, W. Wang, L. Li, G. Perry, H.G. Lee, X. Zhu, Oxidative stress and mitochondrial dysfunction in Alzheimer's disease, Biochim. Biophys. Acta 1842 (2014) 1240–1247.
[72] U. Dettmer, A. Newman, F. Soldner, E.S. Luth, N.C. Kim, V.E. von Saucken, J.B. Sanderson, R. Jaenisch, T. Bartels, D. Selkoe, Parkinson-causing α-synuclein missense mutations shift native tetramers to monomers as a mechanism for disease initiation, Nat. Commun. 6 (2015) 7314, http://dx.doi.org/10.1038/ncomms8314.
[73] U. Dettmer, A.J. Newman, E.S. Luth, T. Bartels, D. Selkoe, *In vivo* cross-linking reveals principally oligomeric forms of α-synuclein and β-synuclein in neurons and non-neural cells, J. Biol. Chem. 288 (2013) 6371–6385.
[74] C.H. Westphal, S.S. Chandra, Monomeric synucleins generate membrane curvature, J. Biol. Chem. 288 (2013) 1829–1840.
[75] M.T. Lin, M.F. Beal, Mitochondrial dysfunction and oxidative stress in neurodegenerative diseases, Nature 443 (2006) 787–795.
[76] A. Federico, E. Cardaioli, P. Da Pozzo, P. Formichi, G.N. Gallus, E. Radi, Mitochondria, oxidative stress and neurodegeneration, J. Neurol. Sci. 322 (1-2) (2012) 254–262.
[77] W. Wang, I. Perovic, J. Chittuluru, A. Kaganovich, L.T. Nguyen, J. Liao, J.R. Auclair, D. Johnson, A. Landeru, A.K. Simorellis, S. Ju, M.R. Cookson, F.J. Asturias, J.N. Agar, B.N. Webb, C. Kang, D. Ringe, G.A. Petsko, T.C. Pochapsky, Q.Q. Hoang, A soluble α-synuclein construct forms a dynamic tetramer, Proc. Natl. Acad. Sci. U.S.A. 108 (2011) 17797–17802.
[78] B. Uttara, A.V. Singh, P. Zamboni, R. Mahajan, Oxidative stress and neurodegenerative diseases: a review of upstream and downstream antioxidant therapeutic options, Curr. Neuropharmacol. 7 (1) (2009) 65–74.
[79] V. Shukla, S.K. Mishra, H.C. Pant, Oxidative stress in neurodegeneration, Adv. Pharmacol. Sci. (2011), 572634.
[80] S. Gandhi, A.Y. Abramov, Mechanism of oxidative stress in neurodegeneration, Oxid. Med. Cell. Longev. 3 (2012), 428010.
[81] G.H. Kim, J.E. Kim, S.J. Rhie, S. Yoon, The role of oxidative stress in neurodegenerative diseases, Exp. Neurobiol. 24 (4) (2015) 325–340.
[82] Z. Liu, T. Zhou, A.C. Ziegler, P. Dimitrion, L. Zuo, Oxidative stress in neurodegenerative diseases: from molecular mechanisms to clinical applications, Oxid. Med. Cell. Longev. (2017), 2525967.
[83] G.N. De Iuliis, R.J. Newey, B.V. King, R.J. Aitken, Mobile phone radiation induces reactive oxygen species production and DNA damage in human spermatozoa *in vitro*, PLoS One 4 (2009) e6446, http://dx.doi.org/10.1371/journal.pone.0006446.
[84] M. Tkalec, A. Stambuk, M. Srut, K. Malarić, G.I. Klobučar, Oxidative and genotoxic effects of 900 MHz electromagnetic fields in the earthworm *Eisenia fetida*, Ecotoxicol. Environ. Saf. 90 (2013) 7–12.
[85] A. Campisi, M. Gulino, R. Acquaviva, P. Bellia, G. Raciti, R. Grasso, F. Musumeci, A. Vanella, A. Triglia, Reactive oxygen species levels and DNA fragmentation on astrocytes in primary culture after acute exposure to low intensity microwave electromagnetic field, Neurosci. Lett. 473 (2010) 52–55.
[86] S. Xu, Z. Zhou, L. Zhang, Z. Yu, W. Zhang, Y. Wang, X. Wang, M. Li, Y. Chen, C. Chen, M. He, G. Zhang, M. Zhong, Exposure to 1800 MHz radiofrequency radiation induces oxidative damage to mitochondrial DNA in primary cultured neurons, Brain Res. 1311 (2010) 189–196.
[87] A.M. Marjanovic Cermak, I. Pavicic, I. Trosic, Oxidative stress response in SH-SY5Y cells exposed to short-term 1800 MHz radiofrequency radiation, J. Environ. Sci. Health A Tox. Hazard Subst. Environ. Eng. 53 (2) (2018) 132–138.